Chemical background of contact corrosion between copper and galvanized steel screws

F. Haraszti,[1] L. Trif,[2] Z. May,[2] T. Kovács[1] and J. Telegdi[2,3]*

[1]Óbuda University, Donát Bánki Faculty of Mechanical and Safety Engineering, Institute of Materials and Manufacturing Sciences, Department of Materials Technology, Budapest, Hungary
[2]Research Centre for Natural Science; 1117 Budapest, Magyar tudósok körútja 2, Hungary
[3]Óbuda University, Faculty of Light Industry and Environmental Engineering, Budapest, Hungary
**E-mail: telegdi.judit@ttk.hu*

Abstract

This research aimed to study of the role of galvanic/contact corrosion between copper and galvanized steel screws. Based on our previous investigations by thermal imaging camera under power, the role of corrosion processes around the fitting were in the focus that could be responsible for the heat evolution. In this multi-metallic system where the metals have different electrode potentials, the chemical processes in the presence of electrolyte were analyzed by different, complementary techniques: the weight loss tests measured at different temperatures gave information about the corrosive metal losses, the analyses of metal ions dissolved during the corrosion processes were performed by inductively coupled plasma optical emission spectrometry (ICP-OES), the change in the surface morphology caused by the corrosive deterioration were visualized by stereo microscopy (SM), by scanning electron microscopy (SEM) and by atomic force microscopy (AFM). These complementary experiments proved numerically that during the function of these fittings the copper dissolution was inhibited by the presence of zinc and iron even at increased temperature. The appearance of iron ions in the electrolyte and the brownish spots on the metal surface indicated that first zinc could inhibit the copper corrosion but after the dissolution of the thin zinc layer on the screw, iron takes over the protection of copper.

Received: September 12, 2022. Published: October 29, 2022 doi: 10.17675/2305-6894-2022-11-4-1

Keywords: *bi- and multi-metallic corrosion, copper, galvanized steel screw, weight loss tests, ICP-OES, surface morphology visualization by SEM and AFM.*

1. Introduction

The metal corrosion that could be chemical, electrochemical and microbiologically influenced is an undesired material deterioration. Generally it could be caused by aggressive chemicals (acids, alkali), by the presence of electrolytes or corrosion relevant microorganisms as well as by the common presence of different metals.

The metals can be dissolved in an anodic process by losing electrons:

$$\mathrm{Me} \leftrightarrow \mathrm{Me}^{n+} + n\mathrm{e}^{-}$$

where Me indicates the solid metal, Me^{n+} is the dissolved metal ion and n is the charge transfer number of electrons in wet environment. It is well-known that during the corrosion process energetic/heat changes take place without outer electric polarization. The free electrons are consumed in a cathodic process:

$$\mathrm{Ox} + n\mathrm{e}^{-} \leftrightarrow \text{red prod.}$$

These two reactions go in parallel.

In our experimental conditions bi- and multi-metallic contact corrosion is discussed, which is a special form of the galvanic corrosion [1–3].

The electrical potentials of metals are different, that could be quantified in the presence of conductive media (humid air, moisture, water, saltwater). Before combination of different metals it is important to know their electric potentials and to determine the possibility of galvanic corrosion by the corrosion potentials in the presence of electrolyte that allows the connection between the metals. The transfer of electrons from one metal to other results in electric current and causes accelerated corrosion of that metal that loses electrons while the other one that receives electrons is preserved. The galvanic cells needs an anode (metal with greater negative electric potential, electrons are cumulated here, the corrosion is accelerated), a cathode (metal with less negative electric potential, here are the electrons consumed, the metal is protected from corrosion), and an electrical connection by electrolyte that transfers the electrons from the anode to the cathode.

When all these conditions are present at the same time the less noble anode deteriorates at accelerated rate. The differences in electrical potential and the aggressiveness of the electrolyte are the main factors that determine the corrosion rate. The current that will flow from the less noble metal to the nobler one, will cause the oxidation of the less noble metal [4–6].

The galvanic corrosion causes located metal dissolution, and is limited to the contact zone [7].

To avoid or diminish the contact corrosion rate it is necessary to keep in mind to choose the right combination of metals.

Galvanized steel and copper are commonly used in transmission and distribution power lines.

In our case copper and galvanized steel were in contact and the evolved heat affected the corrosion of the metal set. The characteristic standard potential of the three metals in experiments are the follows [V]: copper: +0.344; iron: –0.441; zinc: –0.762; galvanized steel: –1.00.

As previously the importance of the potential differences was mentioned, it is clear that when, in the present of electrolyte, zinc is in contact with copper in the presence of electrolyte, the galvanic reaction will lead to dissolution of the zinc. In our case the

galvanized steel screw contacts the copper shoe. The zinc protects steel from rusting by a slow current flow from the zinc to the iron in the steel, but the zinc can establish current with other contacting metals, in our case this is the copper. In the first experimental period iron cannot contact copper (because of the thin zinc coating). The first reaction is a rapid corrosion of the zinc and only after the dissolution of the zinc from the steel surface can come in juxtaposition with copper.

The potential difference is more significant between the copper and zinc than between the iron and zinc, but the iron also can inhibit the copper dissolution. The stainless steel screws should have round heads and flat seats not to puncture the copper [8].

Our experiments aimed the elucidation of the galvanic corrosion when a copper is in contact with galvanized steel screw. It was already demonstrated that in long-term experiments the corrosion of these metals was accompanied by heat evolution. The only simple method for failure analysis and mode to predict the problems at elevated temperature is the thermographic inspection of heat evolution at the copper /galvanized steel screw/ and female screw connection [9, 10]. By the tests described in this paper the progress of corrosion was followed by different, complementary techniques. The undesired deteriorating processes were accelerated in sodium chloride solution in order to model the long-term operation in a shorter time.

2. Materials and Methods

2.1. Metals

The fitting used in the corrosion tests consisted of copper (non-insulated, long ring tube terminal, composition: 99.5% Cu) and galvanized, hexagonal head threaded steel screw and female screw fastener (medium carbon steel 8.8, quench and tempered [11]; its composition [%]: C: 0.25–0.55, Mn: 0.25; Si: 0.035, P: 0.035, S: 0.00, covered by thin Zn layer.

These metals have several benefits (*e.g.* high tensile strength, high corrosion resistance, *etc.*) and are used in various industrial applications.

Figure 1. Composition of carbon steel 8. Metal pieces under investigation.

2.2. Electrolyte

The electrolyte in the corrosion tests was aqueous sodium chloride solution (3%).

2.3. Weight loss test

After measuring the weight of the degreased copper and galvanized steel screws they were dipped separately as well as together in the test tubes containing NaCl solutions of 3% for 91 hours. The experiments were carried out at different temperatures: 23°C, 40°C, 60°C and 80°C in order to simulate the industrial conditions when the corrosion enhances the temperature of the multi-metallic system in the tenure of usage. After running out the experimental time, the metals were pulled out from the solution; were washed with distilled water and then the rust layers were removed by a special solution (10% HCl with 100 ppm hexamethylene tetramine). All metal species were washed again with water, then by acetone and after letting them to dry on air their weight was measured again. The difference between the initial and final weights showed how seriously the metals were corroded.

2.4. Metal ion concentration analysis after corrosion test

The metal ions dissolved in the NaCl solutions in the corrosive environment were measured by inductively coupled plasma – optical emission spectrometry (ICP-OES); it can measure about 30 elements at the same time, at the concentration range from even μg/L up to high percent levels; the plasma is very stable due to the special operating frequency and broad band-width, which is equipped by a CCD detector (that makes possible to cover the wavelength range of 175–775 nm). The instrument used in our experiments was a Spectro Genesis ICP-OES spectrometer (with axial plasma observation).

2.5. Visualization of the morphological conditions

Morphological changes caused by contact corrosion were visualized by scanning electron-microscope (SEM) and by atomic force microscope (AFM).

2.5.1. SEM

Focused electron beam with very low wavelength scans the surface and produce signals on the interaction of kinetic energy of electrons with the solid surface molecules. The evolved secondary (and backscattered) electrons produce an image about the solid surface and allow the visualization of the surface morphology before the start and after the end of the corrosion tests in the range of some tens of nm and some of hundreds μm. The metal surfaces were gold coated. (Zeiss Evo 40 scanning electron microscope operated at 10 kV.)

2.5.2. AFM

The atomic force microscope allows the visualization of a solid surface in the range of μm and nm, on air, without any surface pretreatment. It measures the force (nN/m) between a very sharp tip and the solid surface. This technique can inform us not only on the morphology of the solid surface but gives numerical information about the surface roughness (Digital Instrument, NanoScope III).

3. Results and Discussion

The time-dependent thermographic and the visual observation of heat evolution at the copper/galvanized steel screw/ and female screw connection in use proved that the heat evolution is due to corrosion processes.

3.1. Pilling–Bedworth ratio

Before the demonstration of results of different corrosion test, it was necessary to survey the structure of the different oxide layers that can cover the copper, zinc and iron surfaces. The best is to study the Pilling–Bedworth (R_{PB}) ratio that characterizes the differences between the metal and metal oxide volume. These characteristics could be calculated with the following equation:

$$R_{PB} = \frac{V_{\text{metal oxide}}}{V_{\text{metal}}} = \frac{M_{\text{metal oxide}} \cdot \rho_{\text{metal}}}{n \cdot A_{\text{metal}} \cdot \rho_{\text{oxide}}}$$

where:

$V_{\text{metal oxide}}$ – volume of elementary cell of metal oxide;
V_{metal} – volume of elementary cell of metal;
n – number of metal atoms in the oxide;
ρ – metal density;
M – molar mass;
A – atomic mass.

The R_{PB} values define the structure of the oxides formed on metal surface. The possible cases are the follows:

The oxide layer is thin, not continuous; there is no protective effect:

$$R_{PB} < 1$$

The oxide layer can save the metal surface from the further oxidation (this is the situation in the case of Ti, Al, and steel with Cr):

$$1 < R_{PB} < 2$$

The oxide layer is very rough, can easily come off in flakes, there is no protection of the metal (this happens in the case of Fe_2O_3):

$$R_{PB} > 2$$

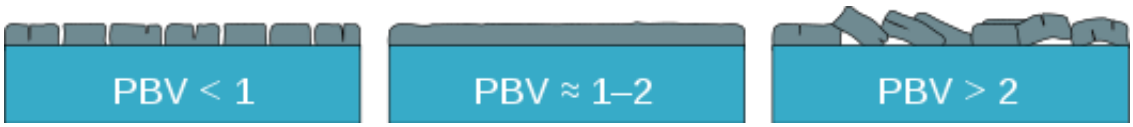

Figure 2. The oxide structures compared to the Pilling–Bedworth ratio [12].

Table 1. The Pilling–Bedworth ratio of different metal oxides [13].

Metal	Oxide	R_{PB}
Zinc	ZnO	1.58
Iron	FeO	1.70
Iron	Fe_3O_4	1.90
Iron	Fe_2O_3	2.14
Copper	Cu_2O	0.75*
Copper	CuO	1.75*

(*calculated by the authors)

The PB values show clearly the Cu_2O layer cannot cover the copper surface uniformly; (though this layer is effective in passivating the corrosion processes) it is not very stable in aqueous chloride solution [14, 15]

The existence of the Cu_2O was proved by photoelectron spectroscopy but these experiments proved that pits start to form on copper surface only then when the copper(I) oxide cannot cover the metal surface continuously. The Cu in higher oxidation state (CuO) forms a smooth, uniform layer. The ZnO oxide layer behaves similarly to the CuO; it also forms a thin covering layer. In the case of iron, the formation of the Fe_2O_3 is purportedly responsible for the detachment, cracking of the oxide layer and for letting visible the pure iron surface.

We wanted to prove by the following experiments that when the galvanized steel of lower electronegativity is in contact with copper, the zinc (and after dissolution of zinc) the iron will be dissolved instead of the copper.

To define numerically the corrosion, complementary experiments were applied to prove and quantify the morphological and heat evolution observations and to show how these phenomena are caused by corrosion products of contacting different metals, and, at the same time, to prove the protecting effect of metals of different electronegativity.

3.2. Results of the weight loss experiments

The next tables summarize the weight losses caused by the presence of electrolyte measured at different temperatures in order to mimic the thermographic experimental conditions.

The weight loss data of galvanized steel screw and copper investigated separately show unequivocally that at higher temperature the corrosive dissolution increases in both cases (metals are used alone or in combination). When the galvanized screw and the copper were applied together, the rate of corrosion (*i.e.* the mass of the dissolved metals) decreased that shows the protecting effect of the galvanized screw at all temperature under investigation.

Table 2. The temperature dependent weight loss results measured on metals dipped separately and together in the NaCl solution of 3%.

Temperature (°C)	Weight loss, Δ*m* (g)		
	Copper	**Galvanized steel screw**	**Copper and screw together**
23	0.0005	0.0057	0.0059
40	0.0012	0.0090	0.0082
60	0.0017	0.0094	0.0106
80	0.0026	0.0184	0.0165

In order to learn more about the corrosive deterioration, the metal ion concentrations in the electrolytes used in weight loss tests were followed by ICP-OES technique that can analyze the metal ions abreast in the same solution.

3.3. Metal ion concentration determination by inductively coupled plasma-optical emission spectroscopy (ICP-OES)

The metal ion concentrations measured in the electrolytes of the weight loss tests are summarized in Table 3.

Table 3. The metal ion concentrations in the corrosive solutions arose at different temperatures, determined by ICP-OES method.

Solution sample	Cu (ppm)	Fe (ppm)	Zn (ppm)
23°C			
NaCl solution, 3%	0.009	0.13	0.058
Copper (alone)	8.40	0.141	0.794
Galvanized screw (alone)	0.16	0.496	170
The two metals applied together	0.20	2.79	126
40°C			
NaCl solution, 3%	0.009	0.13	0.058
Copper (alone)	30.1	2.07	1.21
Galvanized screw (alone)	0.14	53.7	170
The two metals applied together	0.85	107	190

Solution sample	Cu (ppm)	Fe (ppm)	Zn (ppm)
60°C			
NaCl solution, 3%	0.009	0.13	0.058
Copper (alone)	43.6	0.21	3.50
Galvanized screw (alone)	1.06	192	200
The two metals applied together	0.56	159	210
80°C			
NaCl solution, 3%	0.009	0.13	0.058
Copper (alone)	108	0.266	4.77
Galvanized screw (alone)	0.37	904	159
The two metals applied together	0.83	869	134

The ICP-OES data prove that the time-dependent dissolution of copper dipped alone into the electrolyte increases in a large measure: 8.4 ppm at 23°C and 108 ppm at 80°C. On the contrary, when the copper and the galvanized screw are dipped into the sodium chloride solution together, the dissolution of the copper decreases significantly: 0.2 ppm at 23°C, and 0.83 ppm at 80°C. These metal ion values prove the proper, protective function of the zinc and partly the iron metal.

The analysis of solutions whereto the galvanized screw alone and together with the copper shoe was dipped, the increased temperature increase the dissolution of both the iron and zinc metals but there is not significant difference whether the screw was immersed into the electrolyte alone or in combination with copper shoe.

The most important conclusion of both the weight loss measurements and the ICP-OES analyses is that first of all the zinc dissolved from the screw, but when the zinc is mainly in the form of zinc ions in the solution, the iron can take over the protection of the copper even at higher temperature.

3.4. Different microscopic techniques used for investigation of morphological differences caused by corrosion

3.4.1. Surface visualization by SEM technique

The SEM images visualized by the secondary electrons prove univocally the impact of the temperature on the pitting corrosion: at higher temperature the number and size of the pits increases significantly. In cases when the metals were immersed alone into the electrolyte,

the number of pits are much higher than on those samples where they were connected (imitating the real industrial conditions). With other words: in those corrosion experiments when the copper was joined to the galvanized screw and female screw, the number of pits on the copper decreased dramatically. The decrease is best visible on images visualized on samples tested at 80°C. These results support data obtained by ICP-OES measurements: not only had the number of pits decreased but the quantity of the dissolved copper, too.

Table 4. SEM images of different samples visualized at different temperatures.

Sample	**Before the corrosion experiments**
	Temperature 23°C
Copper	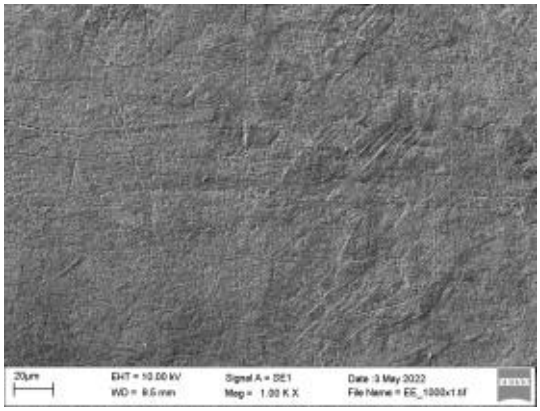
Galv. screw	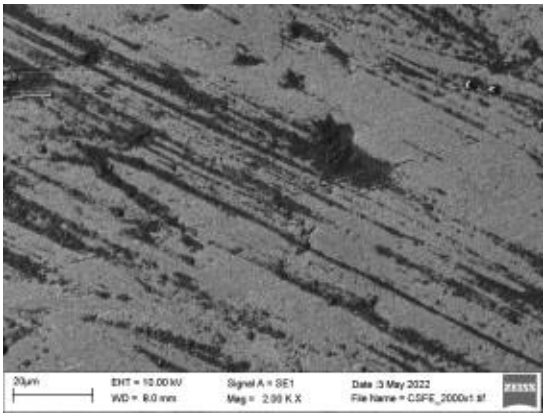
Galv. female screw	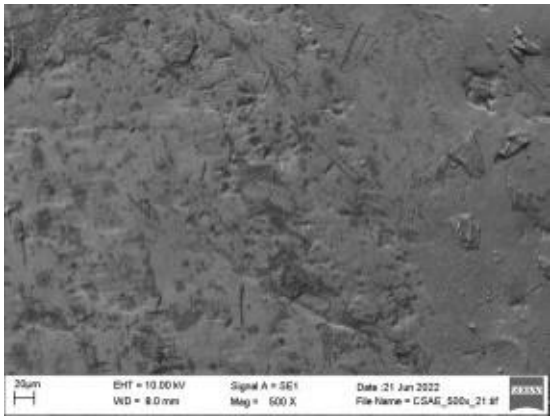

	Samples in the NaCl solution			
Temp.	**23°C**	**40°C**	**60°C**	**80°C**
Copper alone	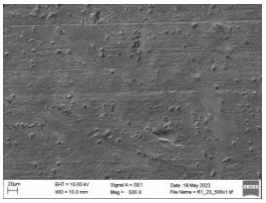	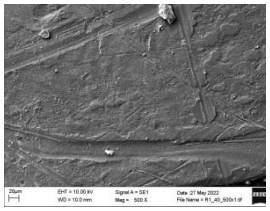	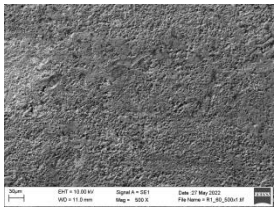	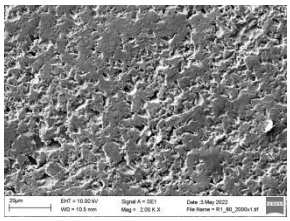
Copper connected to the screw	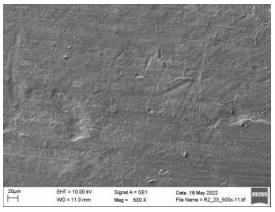	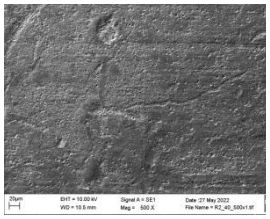	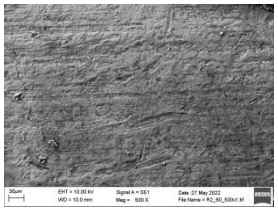	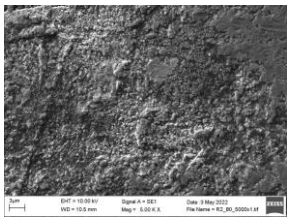
Galv. screw, alone	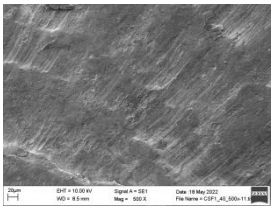	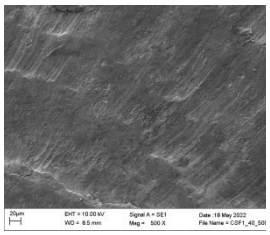	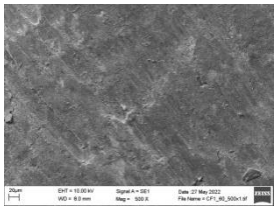	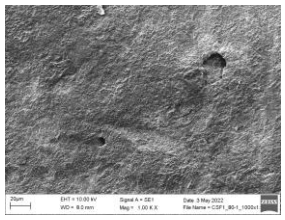
Copper in contact with the screw	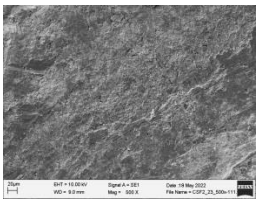	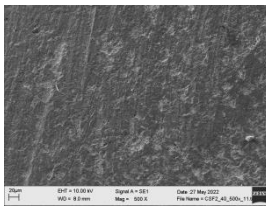	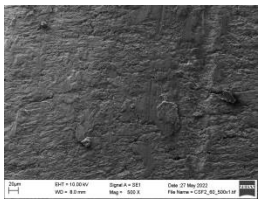	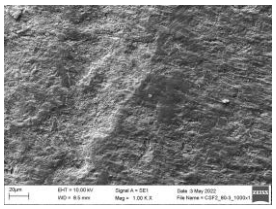
Galv. female screw, alone	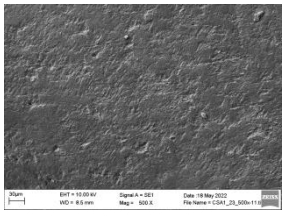	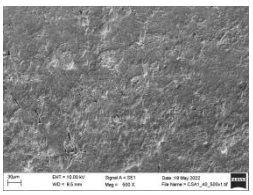	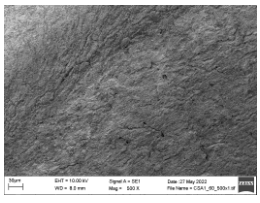	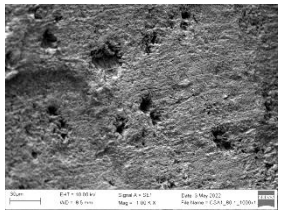
Galv. female screw connected to the copper	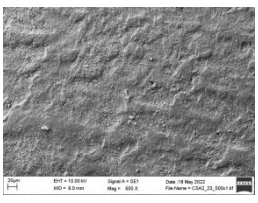	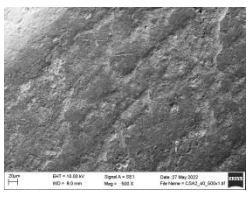	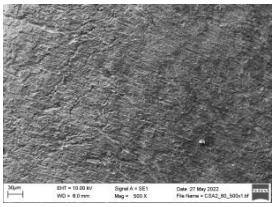	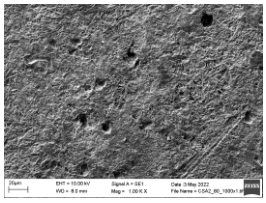

3.4.2. Visualization of the surface morphology by atomic force microscope

The usefulness of the AFM technique in evaluation of corrosive deterioration was already proved earlier [16, 17].

The surface morphologies visualized by AFM technique are summarized in the following Tables.

Table 5. AFM images of metal surfaces (applied separately) before and after dipping them into corrosive electrolyte. The scanned metal surfaces are: 5×5 μm. The surface height difference values (Δ*vm*) are summarized in Table 7.

Galv. screw (alone)	**Its section**
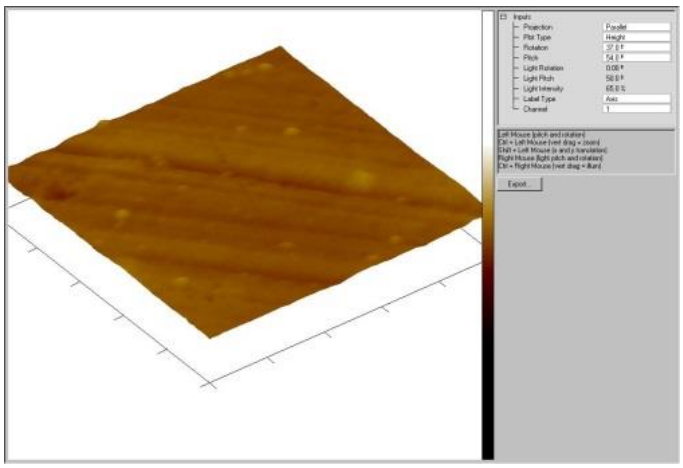	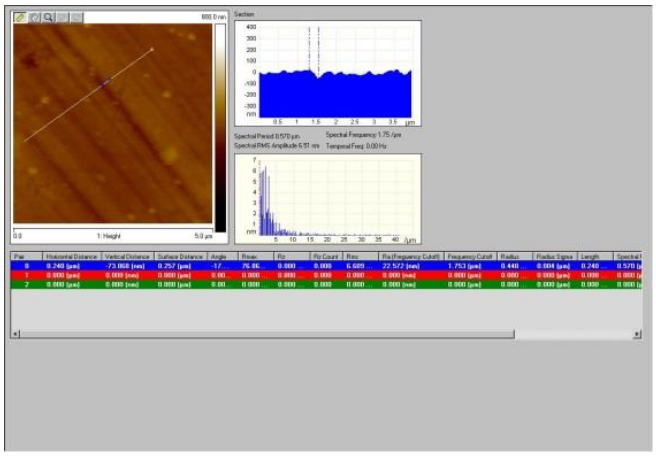
Galv. screw (alone) in 3% NaCl for 2 h (1st place)	**Its section**
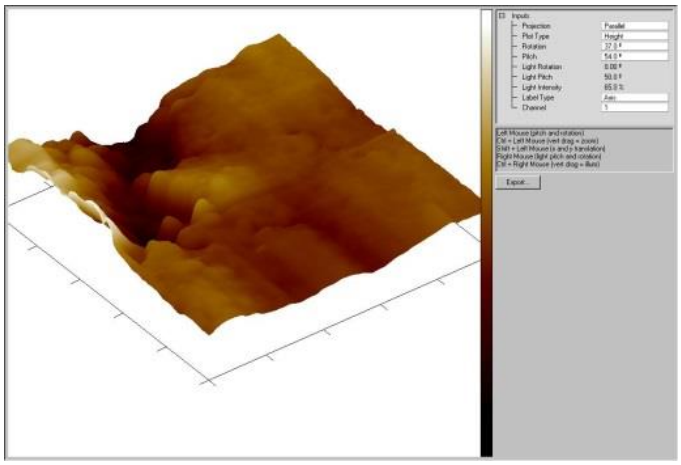	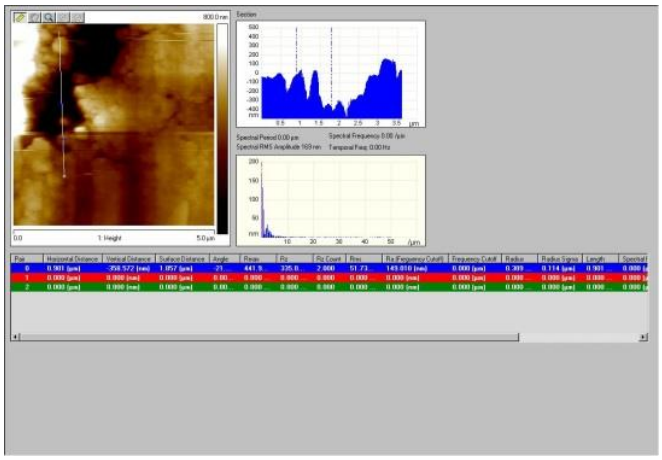

Galv. screw (alone) in 3% NaCl for 2 h (2nd place)

Its section

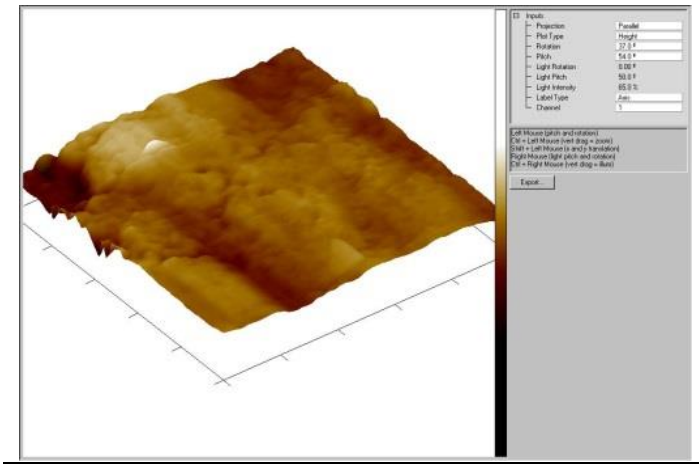

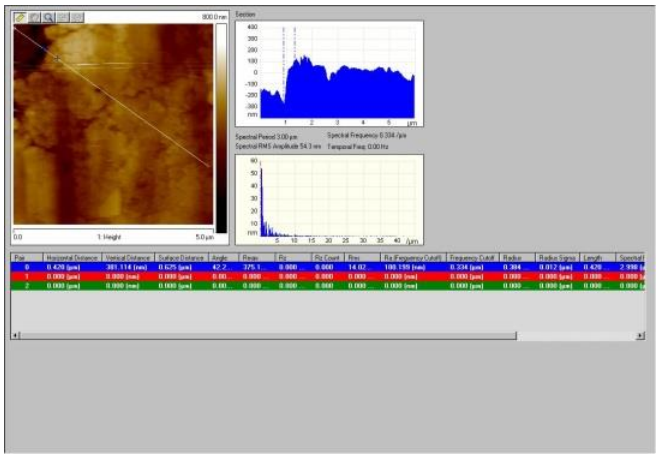

Copper (1st sample)

Its section

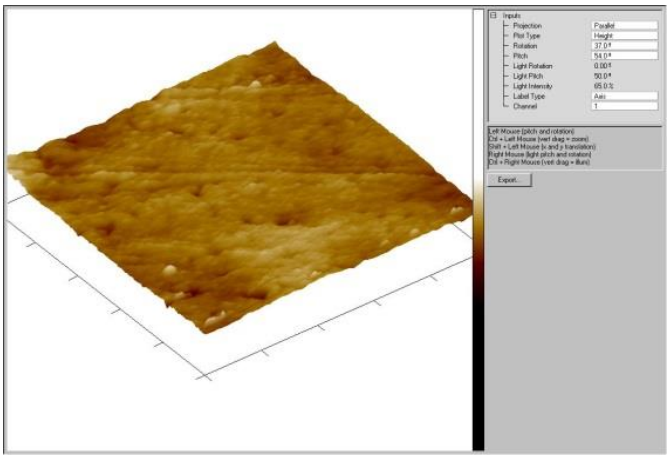

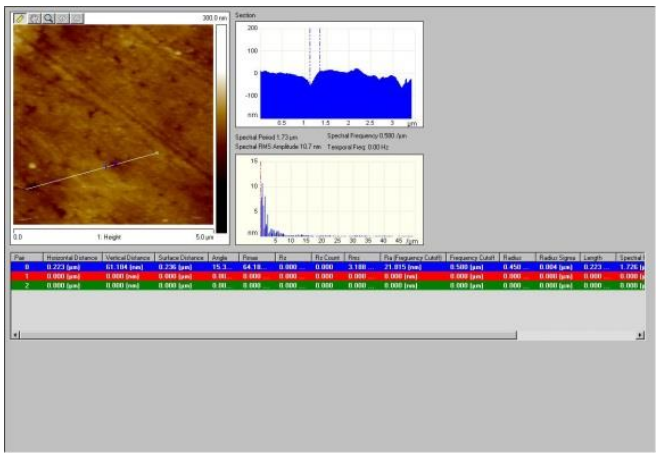

Copper alone (1st sample) in 3% NaCl for 1 h

Its section

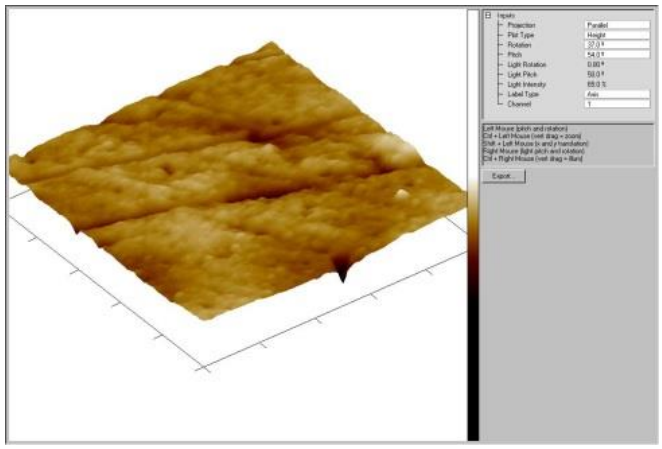

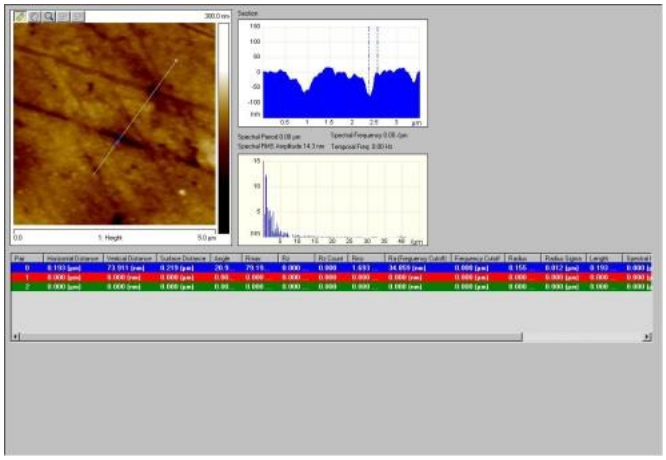

Copper alone (2nd sample)	**Its section**
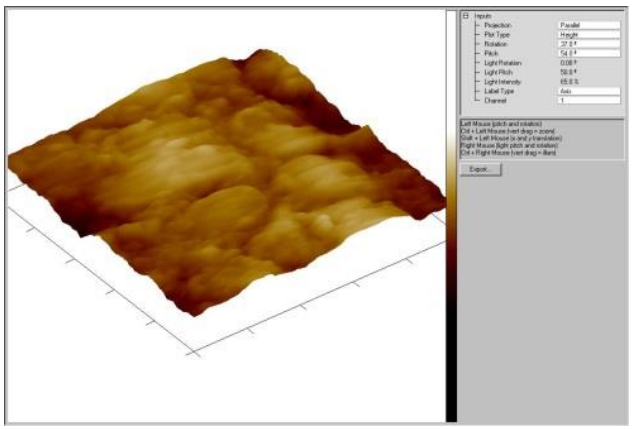	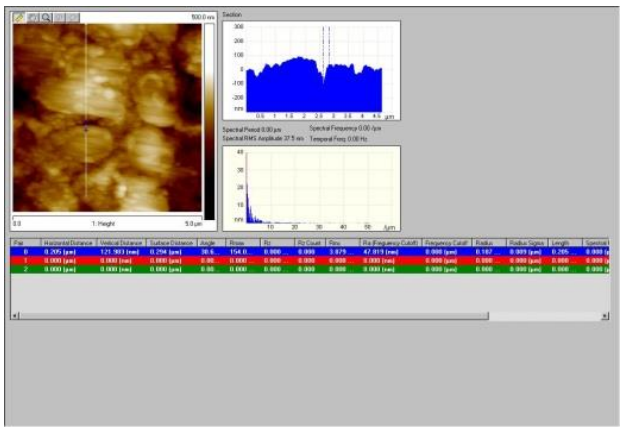
Copper alone (2nd sample) in 3% NaCl for 2h	**Its section**
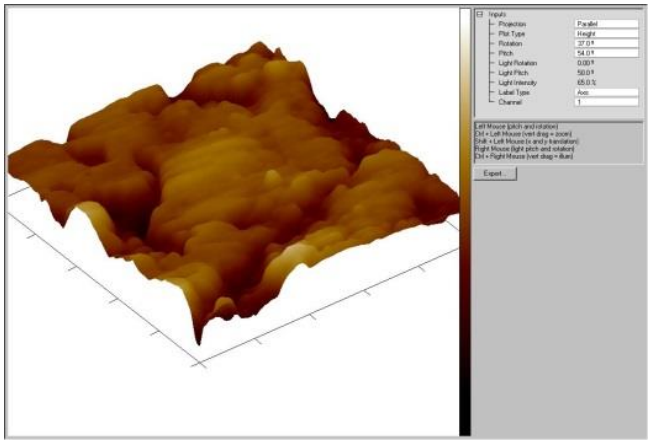	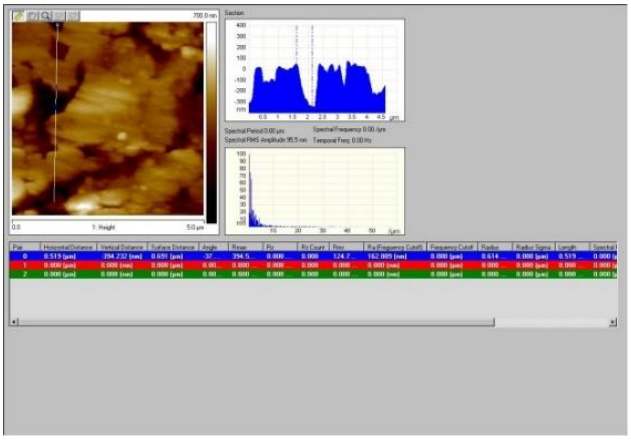

The evaluation of the AFM images, both of the 3D and the section ones, demonstrate that the copper and the galvanized screw suffer serious corrosive deterioration in chloride solution. The visible increased roughness as well as their numerical data together with the Δ*vm* (highest surface differences measured on the section images) are summarized in Table 7 indicate univocally the intensified metal degradation.

The increased corrosion reaction time – demonstrated on copper surface – caused enhanced dissolution of metal proved by the irregular surface.

In order to imitate the real situation, *i.e.* when the copper and the galvanized screws are applied in joined-up form (*i.e.* the individual metals were in close contact and are influenced by the atmosphere with humidity and salts), corrosion experiments were carried out by AFM. In contrast to the previous images, here 2D images are shown as they bear more information about the surface morphology at nanometer scale. The 3D images were the bases for the section that allow studying the numerical values measured on both the galvanized screw as well as on the copper applied in close contact: the high surface difference on the screw dipped into the electrolyte for 1 hour is 135 nm, on the copper 15 nm. For the sake of comparison, when these metals were dipped into the sodium chloride solution separately,

these values were in case of the screw 358 nm and for copper 74 nm. The surface structure of the copper oxide is very interesting; the oxide layer shows a special, regular shape.

Table 6. AFM images of metal surfaces (applied in close contact) after dipping them into corrosive electrolyte. The scanned surfaces: 5×5 in case of the screw and 3×3 μm on copper in order to display the interesting surface patter. The surface height difference values (Δ*vm*) are summarized in Table 7.

Galv. screw in close contact with the copper	**Its section**
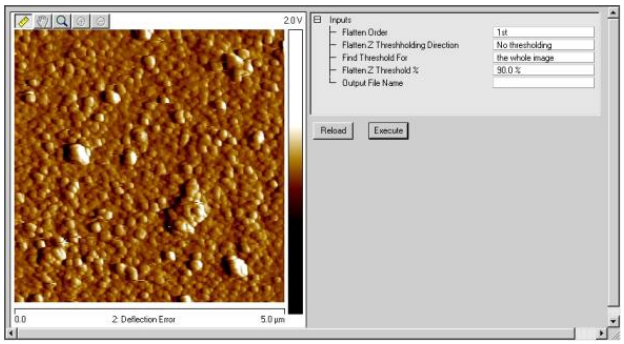	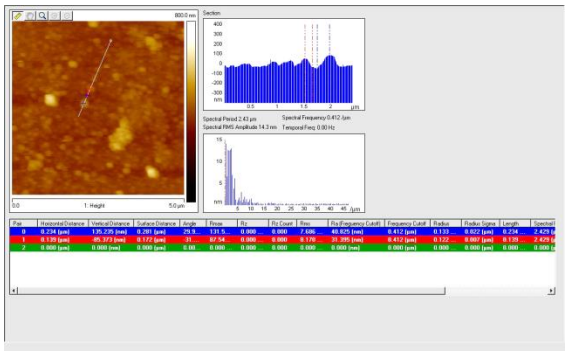
Copper in close contact with galv. screw	**Its section**
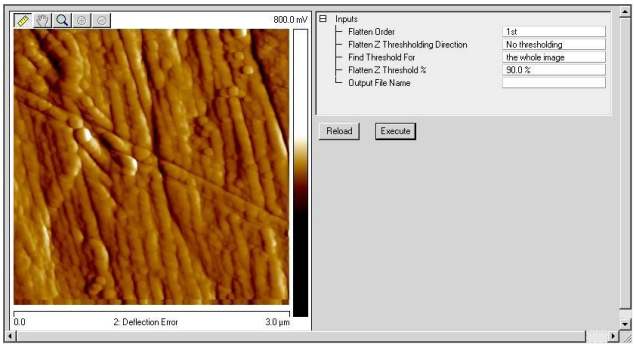	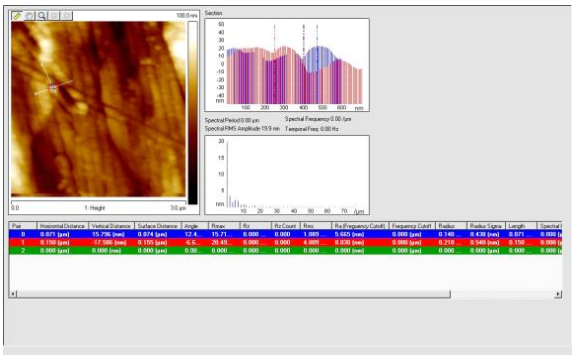

3.4.3. Surface characterization by roughness parameters

The surface roughness plays important role in the characterization of metal properties (*e.g.* adhesion, surface reactivity). The surface will interact with the environment; this explains why its roughness is important. The AFM allows measuring the roughness accurately. It is important to use always the same imaging parameters (scan size, resolution as well as the tip-sample interaction) at measuring the roughness. The mostly applied roughness parameters to characterize surfaces are the follows:

- $\boldsymbol{R_a}$: (roughness average) this is the most commonly used characteristic; it shows the difference between the deepest valley and the tallest peak on the surface. This is one of the most effective surface roughness measure commonly used in the practice. It characterizes the height variation in the surface;
- **Rq**: (or RMS, root mean square roughness) is an average of the profile height deviation from the mean line;

- $\boldsymbol{R_{max}}$: this is the largest single toughness depth within the evaluation length [18, 19].

The quantitative analysis of the AFM images resulted in the following roughness values:

Table 7. The roughness parameters calculated from the AFM images of the metals used alone or in close-contact in the corrosion experiments.

Metals under investigation	R_q (nm)	R_a (nm)	R_{max} (nm)	Δ*vm* (nm)
Copper (1st sample)	10.6	8.12	121	50.0
Copper alone (1st sample) in 3% NaCl for 1 h	14.8	10.7	228	72.5
Copper alone (2nd sample)	48.1	37.6	341	122
Copper alone (2nd sample) in 3% NaCl for 2 h	90.4	68.6	642	394
Galv. screw (alone)	17.4	13.3	177	63.9
Galv. screw (alone) in 3% NaCl for1 h	68.9	52.3	790	381
Copper in close contact with the galv. screw) in 3% NaCl for 1 h	12.0	8.9	89.5	15.8
Galv. screw in close contact with the copper in 3% NaCl for 1 h	30.3	20.5	294	135.2

All the three roughness parameters show that the corrosive environment caused an increase in the surface roughening. In the last column Δ*vm* (the mechanically measured values values) support these tendencies.

When the metals were dipped into the electrolyte in close contact, the vertical distances (Δ*vm*) of the galvanized screw is 135 nm and of the copper shoes 15.8 nm, proving the effective action of the zinc coating on the screw.

Not only the roughness value measured on copper in joined-up position is smaller compared to that one when the copper is applied alone, but this is true for the value got on the galvanized screw, too. This phenomenon explains the importance of the close contact between the metals that does not allow the free flow of the electrolyte, to renew the metal surface and the transfer of the metal ions into the bulk solution. This is reflected on the 2D AFM image taken on the screw where small particles are scattered on the surface as a sign of the corrosion products. The rust formed on the screw surface consists mainly of instable γ-FeOOH with porous structure that change in insoluble Fe_2O_3 product [20].

These experiments were supposed to prove that the corrosion products formed on the multi-metal system decrease significantly the surfaces where the current can flow; this causes in heat evolution in the fitting.

4. Conclusion

The presented work wanted to make clear the problem that arises in the practical life *i.e.* to explain the reason of the warm-up of connected metals with different electronegativity. Copper and galvanized screws were the model metals. In order to clarify the corrosion processes they were immersed into aqueous sodium chloride solution to imitate the reality of the humid environment with different aggressive components, and, at the same time, to increase the corrosion rate. The corrosion was followed by weight loss tests, by analyses of metal ions in the chloride solution and by visualizing the morphological changes caused by the deterioration of the metals by SEM and AFM techniques. Numerical roughness values characterized the roughening caused by the corrosion of metals. The important observations/conclusions are the follows:

- When the copper and galvanized screw were separately immersed into the corrosive solution, the traces of corrosion both in general as well as in pit forms were evidenced by the weight loss test, by the metal ion concentrations analysis and were made visible by SEM and AFM methods;
- Results got by different techniques proved that the dissolution of the copper in the joined-up position is significantly decreased by the presence of zinc on the screw, *i.e.* it was demonstrated that under these experimental conditions the more electronegative metal can save the other with higher electronegativity, i.e. as long as zinc is present, the copper corrosion is largely decreased. When the zinc cannot cover fully the screw surface, the iron takes over the saving task.
- By these experiments the reason of the heat evolution under practical conditions was explained: the corrosion products formed in these experiments do not allow the close contact between the copper and the galvanized steel screw. The zinc (as well as the iron) can decrease the corrosive deterioration of copper only for avail; later the corrosion products will decrease the surface where the current can flow; this is the reason of the heat evaluation.

References

1. S. Szabó, Metal corrosion and its relation to other fields of science, *Int. J. Corros. Scale Inhib*., 2015, **4**, no. 1, 35–48. doi: 10.17675/2305-6894-2015-4-1-035-048
2. N. Ebrahimi, J. Zhang, B. Baldock and D. Lai, Galvanic Corrosion Risk Assessment of Bolt Materials in Contact with ASTM A1010 Steel Bridges, *Corrosion*, NACE International, Houston, 2018.
3. J. Zhang, N. Ebrahimi and D. Lai, Galvanic Corrosion Risk of Using Galvanized A325 Bolts in Corrosion-Resistant Steel Bridges, *J. Bridge Eng*., 2019, **24**, no. 6, 06019001. doi: 10.1061/(ASCE)BE.1943-5592.0001395
4. *Additional Corrosion of Zinc and Zinc Based Alloys Resulting From Contact With Other Metals or Carbon*, British Standards Institution, 1979, 6484.

5. ASTM G82-98(2014), Standard Guide for Development and Use of a Galvanic Series for Predicting Galvanic Corrosion Performance, ASTM International, West Conshohocken, PA, 2014.
6. Ch. Hewitt, A. Humphries and E. Twomey, *Opposites Attract: A Primer On Galvanic Corrosion of Dissimilar Metals*, Modern Steel Construction, 2019.
7. Ch. Vargel, *Corrosion of Aluminium (Second Edition)*, Elsevier Science, 2020. doi: 10.1016/C2012-0-02741-X
8. H. Xue, N. Xu and C. Zhang, Effect of stainless steel on corrosion behavior of copper in a copper-bearing intrauterine device, *Adv. Contracept*., 1998, **14**, no. 2, 153–160. doi: 10.1023/a:1006594818470
9. F. Haraszti, Thermographic Camera Application for Galvanic corrosion detection, *Műszaki Tudományos Közlemények*, 2019, **11**, 77–80.
10. F. Haraszti, Thermographic Inspection in the Electric Industry, *Acta Mater. Transylvanica*, 2018, 1, no. 2, 77–80. doi: 10.2478/amt-2018-0026
11. L. Bull, E. Palmiere, R.P. Thackray, I.W. Burgess and B. Davison, Tensile Behaviour of Galvanised Grade 8.8 Bolt Assemblies in Fire, *J. Struct. Fire Eng*., 2015, **6**, no. 3, 197–212. doi: 10.1260/2040-2317.6.3.197
12. https://en.wikipedia.org/wiki/Pilling/Bedworth_ratio
13. C. Xu and W. Gao, Pilling-Bedworth Ratio for Oxidation of Alloys, *Mater. Res. Innovations*, 2000, **3**, 231–235. doi: 10.1007/s100190050008
14. X. Wei, C. Dong, P. Yi, A. Xu, Z. Chen and X. Li, Electrochemical measurements and atomistic simulations of Cl^--induced passivity breakdown on a Cu_2O film, *Corros. Sci*., 2018, **136**, 119–128. doi: 10.1016/J.CORSCI.2018.02.057
15. A. El Warraky, H. El Shayeb and E. Sherif, Pitting corrosion of copper in chloride solutions, *Anti-Corros. Methods Mater*., 2004, **51**, no. 1, 52–61. doi: 10.1108/00035590410512735
16. T. Abohalkuma and J. Telegdi, Corrosion protection of carbon steel by special phosphonic acid nano-layers, *Mater. Corros*., 2015, **66**, no. 12, 1382–1390. doi: 10.1002/maco.201508304
17. J. Telegdi and T. Abohalkuma, Influence of the nanolayer' post-treatment on the anticorrosion activity, *Int. J. Corros. Scale Inhib*., 2018, **7**, no. 3, 352–365. doi: 10.17675/2305-6894-2018-7-3-6
18. *Surface texture: surface roughness, waviness, and lay*, New York: American Society of Mechanical Engineers, 2020, 144.
19. E.S. Gadelmawla, M.M. Koura, T.M.A. Maksoud, I.M. Elewa and H.H. Sollman, Roughness parameters, *J. Mater. Process. Technol*., 2002, **123**, no. 1, 133–145.
20. X.L. Fan, Y.X. Chen, J.X. Zhang, D.Y. Lin, X.X. Liu and X.J. Xia, Galvanic Corrosion Behavior of Copper–Drawn Steel for Grounding Grids in the Acidic Red Soil Simulated Solution, *Acta Metall. Sin. (Engl. Lett.)*, 2020, **33**, 1571–1582. doi: 10.1007/s40195-020-01071-7

♦ ♦ ♦